Available online at www.sciencedirect.com
SCIENCE DIRECT
Polymer 47 (2006) 1364–1371
polymer
www.elsevier.com/locate/polymer

Preparation and properties of layered double hydroxide/poly(ethylene terephthalate) nanocomposites by direct melt compounding

Wan Duk Lee [a], Seung Soon Im [a,*], Hyung-Mi Lim [b], Kwang-Jin Kim [b]

[a] Department of Fiber and polymer Engineering, College of Engineering, Hanyang University, 17 Haengdang-dong, Seongdong-gu, Seoul 133-791, South Korea
[b] Korea Institute of Ceramic Engineering and Technology, Seoul, South Korea

Received 3 June 2005; received in revised form 12 October 2005; accepted 11 December 2005
Available online 10 January 2006

Abstract

Thermal, rheological and mechanical properties of layered double hydroxide (LDHs)/PET nanocomposites were investigated. To enhance the compatibility between PET matrix and LDHs, organic modification of parent LDH having carbonate anion was carried out using various anionic surfactants such as dodecylsulfate (DS), dodecylbenzenesulfonate (DBS), and octylsulfate(OS) by rehydration process. Then, PET nanocomposites with LDH content of 0, 1.0, and 2.0 wt% were prepared by direct melt-compounding. The dispersion morphologies were observed by transmission electron microscopy and X-ray diffraction, indicating that LDH-DS were exfoliated in PET matrix. From the rheology study, there are some network structures owing to filler–filler and/or filler–matrix interactions in nanocomposite systems. Consequently, DS intercalated LDH provided good compatibility with PET molecules, resulting in exfoliated LDH-DS/PET nanocomposites having enhanced thermal and mechanical properties as compared to other nanocomposites as well as homo PET.

Keywords: Layered double hydroxides (LDH); Nanocomposites; Direct melt compounding

1. Introduction

In last decades, much of attentions have been concentrated to the study of nanocomposites built from inorganic layered materials and a polymer. The most important factors for this research area are (1) dispersion of inorganic nanoparticles in polymer matrix and (2) compatibility between inorganic filler and organic polymer. These two main researching approaches on the nanocomposites could lead to a goal of improved properties such as mechanical property, thermal stability and gas permeability. Lots of investigations on such nanocomposite systems have been focused on the assembly of polymer with cationic clay [1]. However, layered double hydroxides (LDH), so called anionic clay, for such systems have been received less attentions. Some intercalation study of polymers into the LDHs have been investigated so far [2,3]. These studies, however, did not concern the physical properties of nanocomposites or the dispersion of LDHs in the polymer matrix, which could be one of the most important properties of nanocomposites. Recently, the study on the LDH nanocomposites with polyimide [4], epoxy [5], and LDPE [6], concerning physical properties and dispersion, has been reported. However, PET nanocomposites using anionic LDHs have not been reported up to the present.

Layered double hydroxides (LDH) are brucite-like layer materials, having anionic counter ion in the gallery space [7]. The positive layer charge is originated by the substitution of the divalent cation by trivalent one. In order to attain electroneutrality, an appropriate number of anions must incorporate into the interlamellar domain. Their general chemical formula is $[M^{2+}_{1-x}M^{3+}_{x}(OH)_2]^{x+}A^{m-}_{x/m}\cdot nH_2O$, where M^{2+} is a divalent cation, M^{3+} is a trivalent cation and A is an interlamellar anion with charge $m-$. The important application field for anionic clays are catalysts, anion exchangers, absorbents, medicinal applications [7–14]. Hydrotalcite, a naturally occurring LDH with carbonate anion, is the representative example for the LDH having the formula $Mg_6Al_2(OH)_{16}(CO_3)^{2-}\cdot 4H_2O$.

To apply anionic LDH to nanocomposite system, preparation of organo-modified LDH resulting in an increase of in gallery spacing is very important because inorganic LDH and organic polymer matrix are basically incompatible. In the past 20 years, many reports about the intercalation of organic anions into LDHs have been discussed [4,5,15]. Crepaldi et al. [15] reported organo-modified LDH which was intercalated by

* Corresponding author. Tel.: +82 2 2220 0495; fax: +82 2 2297 5859.
E-mail address: imss007@hanyang.ac.kr (S.S. Im).

0032-3861/$ - see front matter © 2005 Elsevier Ltd. All rights reserved.
doi:10.1016/j.polymer.2005.12.056

surfactant such as dodecylsulfate (DS) and dodecylbenzenesulfonate (DBS), resulted in increased basal spacing up to 29 Å. If we use surfactant-intercalated LDHs for nanofillers of composite system, monomers or polymer chains can easily incorporate into LDH gallery space because of not only enlarged gallery spacing but also improved hydrophobic nature of LDH nanolayers, resulting in increased mechanical and thermal properties.

The aim of the present work is to investigate the effects of various organo-modified LDHs on thermoplastic PET polymer. PET nanocomposites were prepared by conventional melt compounding, which would be more economical and simple method than in situ polymerization. Then, thermal and mechanical properties, dynamic rheological behaviors and morphologies for the nanocomposites were investigated and discussed in detail.

2. Experimental

2.1. Preparation of organo-modified LDHs

The parent LDH (hydrotalcite, MGALCO3) with Mg/Al ratio = 3 was kindly supplied from KICET, Korea. There are various routes for the synthesis of organo-modifed LDH such as ion-exchange reaction, coprecipitation method and rehydration of calcined oxide. The efficiency of anion exchange in LDHs is considerably high. Bish [16] reported efficiencies very close to 100% for the exchange of carbonate in acid medium. However, low pH values must be required to achieve such high ion exchange efficiency, leading to a partial decomposition of the layers. In present study, rehydration method was therefore conducted. The nature of LDH decomposition during the calcination has been widely investigated, and it has been reported that reconstruction of the calcined material to pure LDH is possible by rehydration process [17–19]. To make calcined precursor oxide (MGALCAL), MGALCO3 was calcined in air at 500 °C for 6 h. 0.2 mol amount of sodium dodecylsulfate (DS), sodium octylsulfate (OS) and sodium dodecylbenzenesulfonate (DBS) were added into each 200 ml of deionized water with stirring under nitrogen purge, and maintained the temperature of 65 °C for 1 h. DS (≥98%), OS (≥95%) and DBS (≥98%) were purchased from Sigma Aldrich, and used as received. A 2 g of MGALCAL was then added into the each aqueous solution, and the mixture stirred vigorously for 3 h. The pH of the solution was stabilized to a value of 10. The resultant product was isolated by repeated filtration and washing with deionized water, and dried under vacuum at room temperature.

2.2. Preparation of PET nanocomposites

Poly(ethylene terephthalte) (PET), having 0.655 dl/g of intrinsic viscosity, was kindly supplied from Toray–Saehan Co. Ltd. PET nanocomposites were prepared by direct melt compounding method using Haake minilab twin co-rotating screw extruder at various mixing conditions such as filler type (MGALCO3, MGALDS, MGALDBS, MGALOS) and filler content (0, 1.0, 2.0 wt%). The compounding was carried out under a barrel temperature of 270 °C, roll speed of 200 rpm, and average residence time of 60 s. All materials were dried in vacuum oven at 75 °C for 24 h prior to use.

2.3. Characterizations

The X-ray diffraction measurements were carried out on a Rigaku Denki X-ray generator (Rigaku model D/MAX-2500) using CuK_α radiation operated by 40 kV and 100 mA. The scan angle covered $1.5° < 2\theta < 70°$ for LDHs and $1.5° < 2\theta < 16°$ for nanocomposites (2θ is scattering angle, θ is Bragg angle) at a speed of 3°/min. In order to verify the physicochemical properties of each LDHs, Fourier transform infrared (FT-IR) analysis was conducted using Nicolet 760 MAGNA-IR spectrometer.

The thermal properties of nanocomposites were measured using Perkin–Elmer DSC-7 instrument, previously calibrated with indium and zinc. To remove previous thermal history, all samples were first heated at 280 °C for 3 min and then quenched to 30 °C at a rate of 500 °C/min. Then the second scanning of heating and cooling run was performed at a rate of 10 °C/min. The thermogravimetric analysis (TGA) for thermal stability of nanocomposites was performed under air purge at a heating rate of 10 °C/min using TA instrument SDT 2960. The rheological properties of nanocomposite melts were measured by advanced rheometric expansion system (ARES, Rheometric scientific Inc.) with the parallel plate geometry. The frequency was ranged from 0.05 to 500 rad/s with a 12.5 mm diameter parallel plate of 1.0 mm gap at 270 °C. The dispersion morphology of LDHs in PET matrix were examined by transmission electron microscope (JEOL 2000FX, operated at 200 kV). Ultra-thin sections for TEM analysis were prepared by using a diamond knife at a temperature of −40 °C. Mechanical test were conducted with the tensile testing machine (Instron 4465, Instron Corp.) with a crosshead speed of 10 mm/min at 50 °C.

3. Results and discussions

Fig. 1 shows FT-IR spectra of the LDHs modified with various surfactants as well as raw LDH containing carbonate anion. A broad absorption peak between 3600 and 3000 cm^{-1} is assigned to O–H group stretches of both hydroxide layers and the interlayer water as shown in Fig. 1(a). As the anions having long alkyl chains such as dodecylsulfate (DS), octylsulfate (OS), and dodecylbenzenesulfonate (DBS) are absorbed into interlayers and surfaces of hydroxide layers during rehydration process, strong absorption peaks of asymmetric and symmetric CH_2 are appeared at 2945 and 2845 cm^{-1}, respectively. In Fig. 1(b), furthermore, the peak of carbonate ion complexes for MGALCO3 is decreased at around 1380 cm^{-1}, while peaks of sulfate ion complexes for MGALDS and MGALOS is increased at around 1220 and 665 cm^{-1}, and those of sulfonate ion complexes for MGALDBS is increased at around 1210 and 665 cm^{-1}. Peaks at 660 and 418 cm^{-1} are associated with Al–O and Mg–O stretching modes in the LDH sheets. To consider the degree of

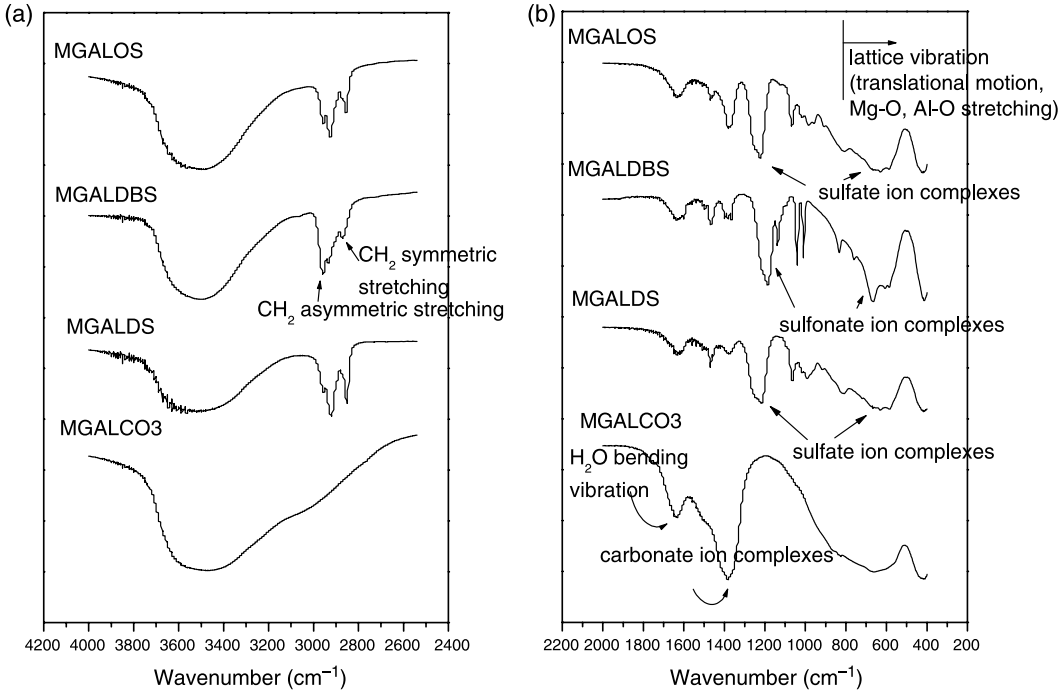

Fig. 1. FT-IR spectra of various LDHs.

intercalation, peak intensity ratio of sulfate or sulfonate ion complex peaks at 1220 or 1210 cm^{-1}, and carbonate ion complex peak at 1380 cm^{-1} to the Mg–O, Al–O stretching peak at 418 cm^{-1} for the peak normalization is summarized in Table 1. As DS and DBS intercalated in LDH layers, I_{1220}/I_{418} and I_{1210}/I_{418} values are increased up to 0.89 and 0.85, respectively, while I_{1380}/I_{418} values are decreased from 1.01 to 0.22, indicating carbonate anions are substituted into sulfonate or sulfate ion during rehydration. On the other hand, OS did not sufficiently substitute carbonate anions from the fact that I_{1380}/I_{418} values decreased only to 0.51. From the FT-IR results, however, it is supposed that alkyl sulfate/sulfonate anions were absorbed in interlayers as well as surface of LDH layers during rehydration process, instead of carbonate anion.

Fig. 2 shows XRD profiles recorded for parent LDH (MGALCO3) and organic anion intercalated LDHs (MGALOS, MGALDS, MGALDBS). The observed data show a basal spacing of 7.8 Å ($2\theta = 11.4°$) for the parent LDH (MGALCO3). After calcinations, MGALCAL do not have characteristic peaks for layered structure as well as Mg/Al layer crystal structures. During the rehydration of calcined LDH with various anionic surfactants, Mg/Al nanolayers are reconstructed from the fact that peaks for (006), (012), and (110) planes are shown at corresponding 2θ angles. As the long alkyl anion incorporates into interlayers during rehydration process, the basal spacing of (003) plane increases significantly, providing evidence that intercalation occurred. The basal spacing of MGALOS, MGALDS and MGALDBS was increased up to 22.6, 26.8, and 28 Å, respectively. It seems that the basal spacings between interlayers are increased with increasing length of alkyl chains for intercalation guest materials. It is supposed that a larger space between Mg/Al nanolayers owing to the intercalation of anionic alkyl surfactants will promote the intercalation of PET molecules as well as increasing compatibility between organo-LDHs and PET molecules, leading to easy exfoliation of the stacking

Table 1
Peak intensity ratio of carbonate and sulfate/sulfonate ion complexes to the Mg–O, Al–O stretching peak

	MGALCO3	MGALDS	MGALDBS	MGALOS
I_{1380}/I_{418}	1.01	0.23	0.22	0.51
I_{1220}/I_{418}	–	0.89	–	0.84
I_{1210}/I_{418}	–	–	0.85	–

I_{1380}, carbonate ion peak; I_{418}, Mg–O, Al–O stretching peak; I_{1220}, sulfate ion peak, I_{1220}, sulfonate ion peak.

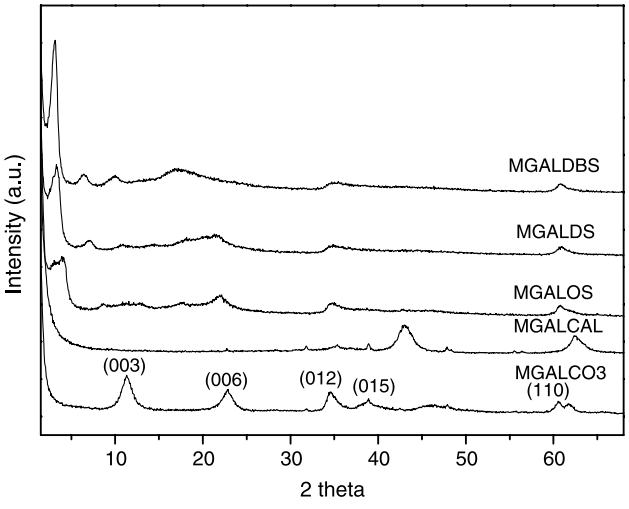

Fig. 2. XRD profiles of various LDHs.

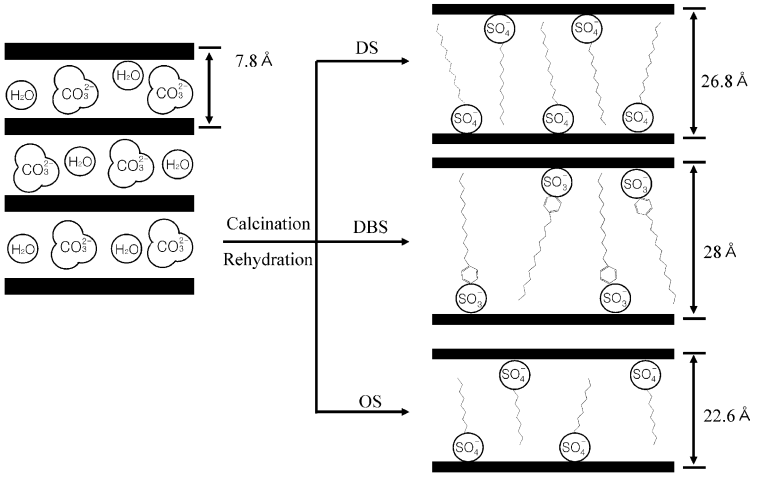

Fig. 3. Schematic diagram of various LDHs.

Mg/Al layers in polymer matrix to form well-dispersed PET/LDH nanocomposites. Expected structure diagram of various LDHs are shown in Fig. 3.

It is noteworthy that LDH feeding level in the preparation of PET nanocomposites was limited by 2 wt% in this study, because PET nanocomposites had become very brittle over the 2 wt% LDH feeding level. This may be attributed to the increase in rigidity of the PET matrix in the presence of reinforcing LDH mineral. Moreover, mechanical, thermal properties as well as rheological properties of PET nanocomposites, discussed later, were effectively influenced by LDHs within 2 wt% loading level. Maximum loading level of LDH in PET matrix was therefore limited to 2 wt% in this study. Fig. 4 shows XRD profiles of PET nanocomposites with various LDHs and loading level of (a) 1.0 wt% and (b) 2.0 wt%. In the case of PET nanocomposites with 2.0 wt% loading of MGALCO3, small (003) reflections (arrow mark) which corresponds to a basal spacing of parent LDH are shown at around 11.2°. It indicates that MGALCO3 particles did not exfoliated by the PET molecules during direct melt-compounding, and aggregate each other retaining its layered structures. It is also confirmed at TEM observation, discussed later. PET nanocomposites with 1.0 wt% of MGALCO3 did not show the characteristic peak for basal spacing but show some noisy peak at around 11.3°. It is supposed that 1.0 wt% of MGALCO3 in PET matrix is too small to detect by bulk XRD apparatus. Otherwise PET nanocomposites with organo-modified LDHs are not shown any peaks for a basal spacing of LDHs, indicating exfoliation of LDH interlayer structures in PET matrix. From XRD results, it is anticipated that increased basal spacing and hydrophobicity of Mg/Al nanolayers owing to the intercalation of anionic alkyl surfactants promoted easy

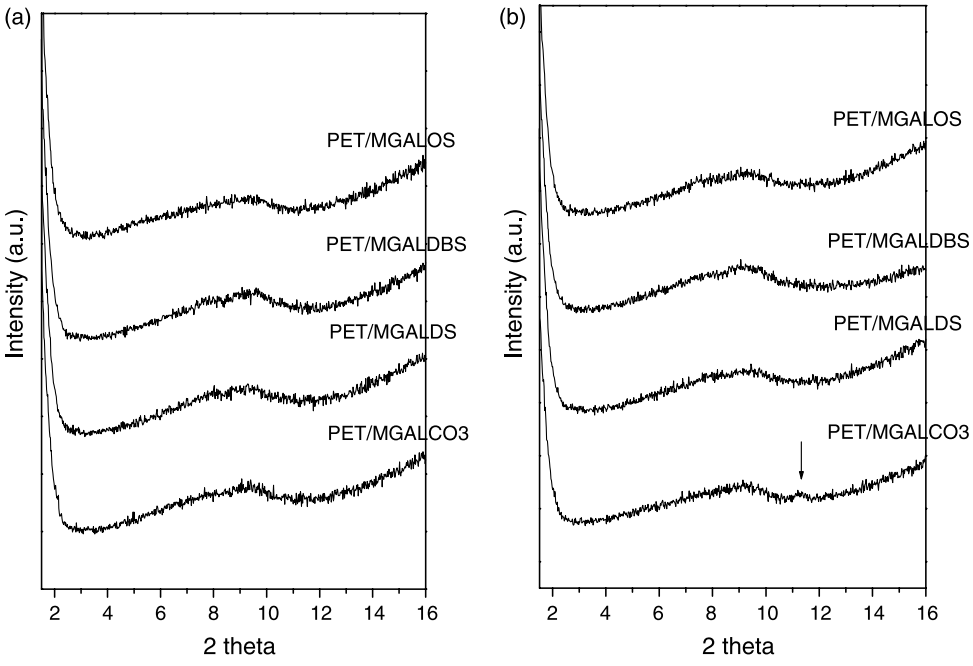

Fig. 4. XRD profiles of PET nanocomposites with (a) 1.0 wt% and (b) 2.0 wt% LDH content.

exfoliation of the stacking LDH layers during direct melt-compounding, resulting in well-dispersed PET/LDH nanocomposites. However, XRD results cannot be the absolute evidence for the nanolayer exfoliation, because XRD apparatus detect diffractions came from overall sample area irradiated by X-ray. If LDHs was intercalated and exfoliated partially in the PET matrix, and if partially exfoliated LDH with small size of stacks did not have sufficient well-defined layered structures for the X-ray diffraction, then LDHs characteristic diffractions for the basal spacing cannot be detected by bulk XRD apparatus. Moreover, if the basal spacing between layers was enlarged owing to the intercalation of polymer molecules, the characteristic peak will shift to the lower angle, beyond the XRD scan range ($<2°$). Therefore, TEM observations have to be accompanied.

Fig. 5 shows TEM images taken from PET nanocomposites containing 2.0 wt% MGALCO3, MGALDS, MGALDBS, and MGALOS. MGALCO3, anticipated to have the least interaction with PET matrix, did not intercalated by PET molecules during melt-compounding, resulting in an image of complete form of layered LDH aggregates as shown in Fig. 5(a). These perfect layer structures can diffract the X-rays, resulting in the peak for the evidence of un-exfoliation in XRD profiles. However, MGALDS was intercalated and/or exfoliated efficiently by PET molecules during direct melt-compounding, and dispersed well in PET matrix (Fig. 5(b)). The nanolayer

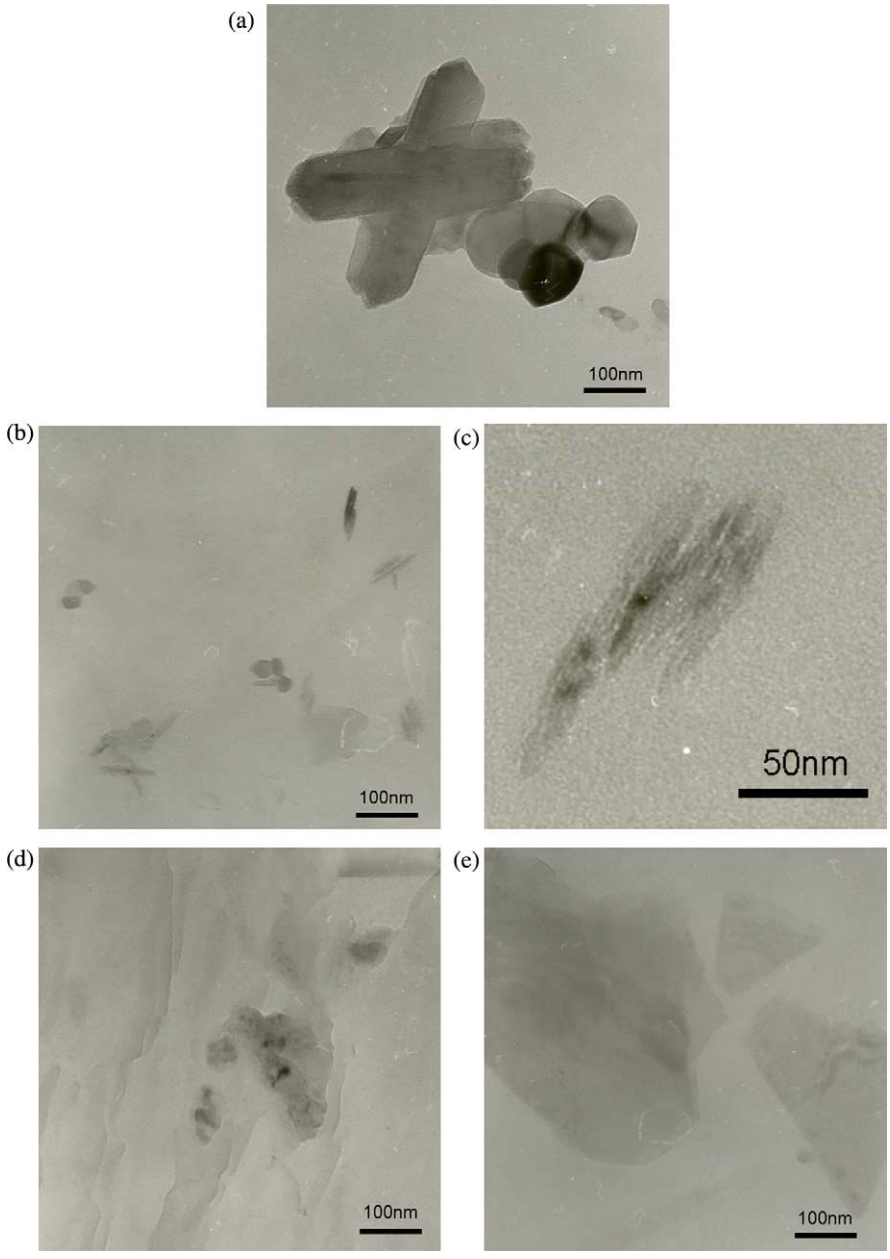

Fig. 5. TEM micrographs of PET nanocomposites containing 2.0 wt% (a) raw LDH, (b) MGALDS (c) MGALDS (high magnification), (d) MGALDBS and (e) MGALOS.

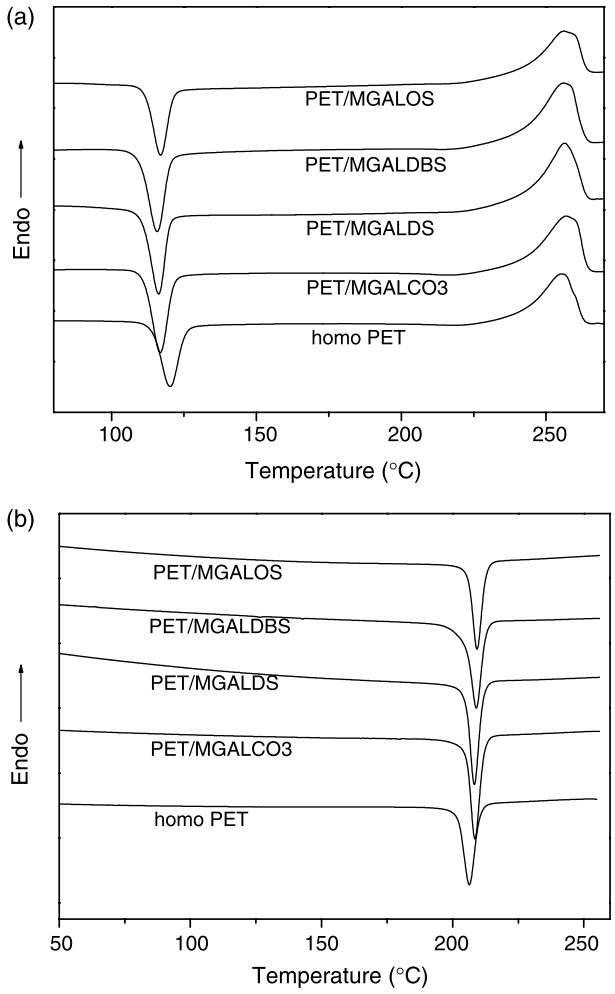

Fig. 6. DSC thermograms of 2.0 wt% LDH/PET nanocomposites during (a) heating and (b) cooling run.

thickness was almost 5–8 nm as shown in Fig. 5(c). Though the MGALDBS and MGALOS were also confirmed to the exfoliation by XRD, some aggregates were observed as shown in Fig. 5(d) and (e), which could affect negatively in PET bulk properties. It is anticipated that because rigid junction point of DBS owing to the rigid benzene rings and shorter length of OS could make exfoliation difficult, partial exfoliation of MGALDBS and MGALOS occurred resulting in the formation of some small aggregates in PET matrix.

DSC thermograms for 2.0 wt% LDH/PET nanocomposites during heating and cooling run are shown in Fig. 6 and the results of DSC are summarized in Table 2. The crystallization temperature during heating (T_{ch}) decreased and the degree of super cooling (ΔT) on the cooling scans (Fig. 6(b)) decreased in all nanocomposites, indicating that LDH nanofillers act as nucleating agent of crystallization and accelerate the crystallization rate of PET matrix. These behaviors are similar to the results reported for the general nanocomposites prepared by direct melt-compounding [20]. However, the melting peaks (T_m) of all nanocomposites on the heating scans (Fig. 6(a)) are almost same as homo PET regardless of the LDHs type. It is supposed that because LDH nanofillers cannot affect PET crystal perfection and/or size, but affect only in crystallization rate of PET acting as a nucleating agent, endothermic peak temperature of all nanocomposites are almost same as homo PET.

A typical thermogravimetric curves for 2.0 wt% LDH/PET nanocomposites are presented in Fig. 7 and the results of TGA are summarized in Table 2. Fig. 7 shows that PET nanocomposites with MGALDS and MGALDBS are more stable up to high temperature than homo PET, and draw the similar weight loss curves and slopes. The temperature at weight reduction of 2 and 5% (T_D^2 and T_D^5) for PET nanocomposites with MGALDS and MGALDBS in Table 2 are also held higher temperature than homo PET. The reason for these results is that the exfoliated nanolayers of MGALDS obstructed the internal diffusion of intense heat and various gaseous substances that formed during pyrolysis of PET. In the case of MGALDBS, it is anticipated that benzene rings in DBS unit also can assist the thermal stability of nanocomposites in spite of presence of some unexfoliated stacks as already shown in Fig. 5(d). On the other hand, thermal stability of PET nanocomposites with MGALCO3 and MGALOS is similar to that of homo PET. It is supposed that MGALCO3 and MGALOS in PET matrix could not act as obstacles for those heat and gases, because stacked nanolayers of MGALCO3 and MGALOS were not exfoliated sufficiently during melt-compounding. Especially it is thought that MGALOS was not exfoliated sufficiently, because MGALOS do not have such

Table 2
Thermal properties of PET nanocomposites with various LDHs

Sample		T_m (°C)	T_{ch} (°C)	T_{cc} (°C)	ΔT (°C)	T_D^i (°C)	T_D^5 (°C)
Homo PET		255.7	120	206.4	49.3	351.6	383.4
PET/MGALCO3	1%	255.8	118.9	207.5	48.3	–	–
	2%	257	116.8	208.5	48.5	350.4	386.3
PET/MGALDS	1%	255.7	119.1	208	47.7	–	–
	2%	256.1	116.2	208.2	47.9	351.7	396.4
PET/MGALDBS	1%	255.9	118.8	207.9	48	–	–
	2%	256.2	115.9	208.7	47.5	366.9	394.8
PET/MGALOS	1%	255.8	119.2	208.5	47.3	–	–
	2%	256.1	117	209.1	47	345.8	380.6

T_D^i and T_D^5, the temperature at weight reduction of 2 and 5%.

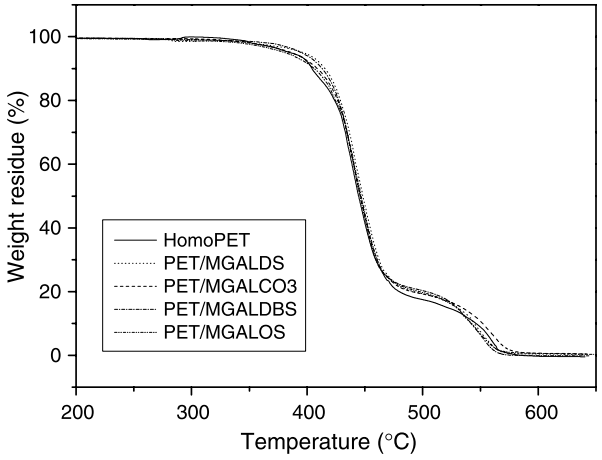

Fig. 7. TGA variations of 2.0 wt% LDH/PET nanocomposites.

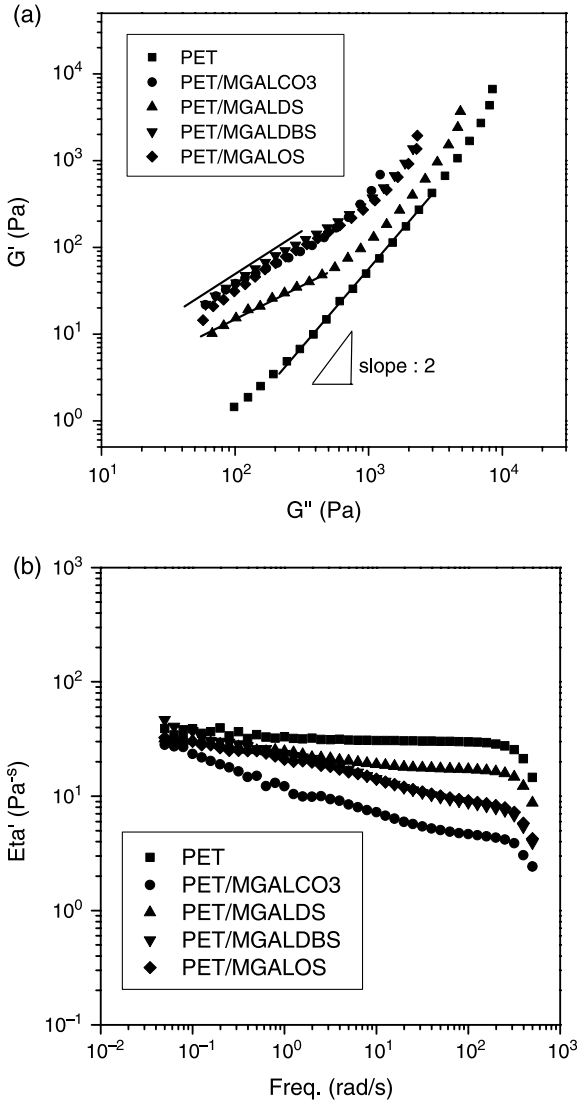

Fig. 8. (a) Cole–Cole plots, and (b) melt viscosity for PET nanocomposites with LDH content of 2.0 wt% at 270 °C.

compatibility with PET molecules owing to the shorter length of OS than DS or DBS, and decreased substitution ratio of octylsulfate anion as shown in FT-IR results.

Rheological properties of PET nanocomposites are shown in Fig. 8. The Cole–Cole plots in Fig. 8(a) show that PET nanocomposites with 2.0 wt% of MGALCO3, MGALDBS, and MGALOS draw similar curves and have low slope of about

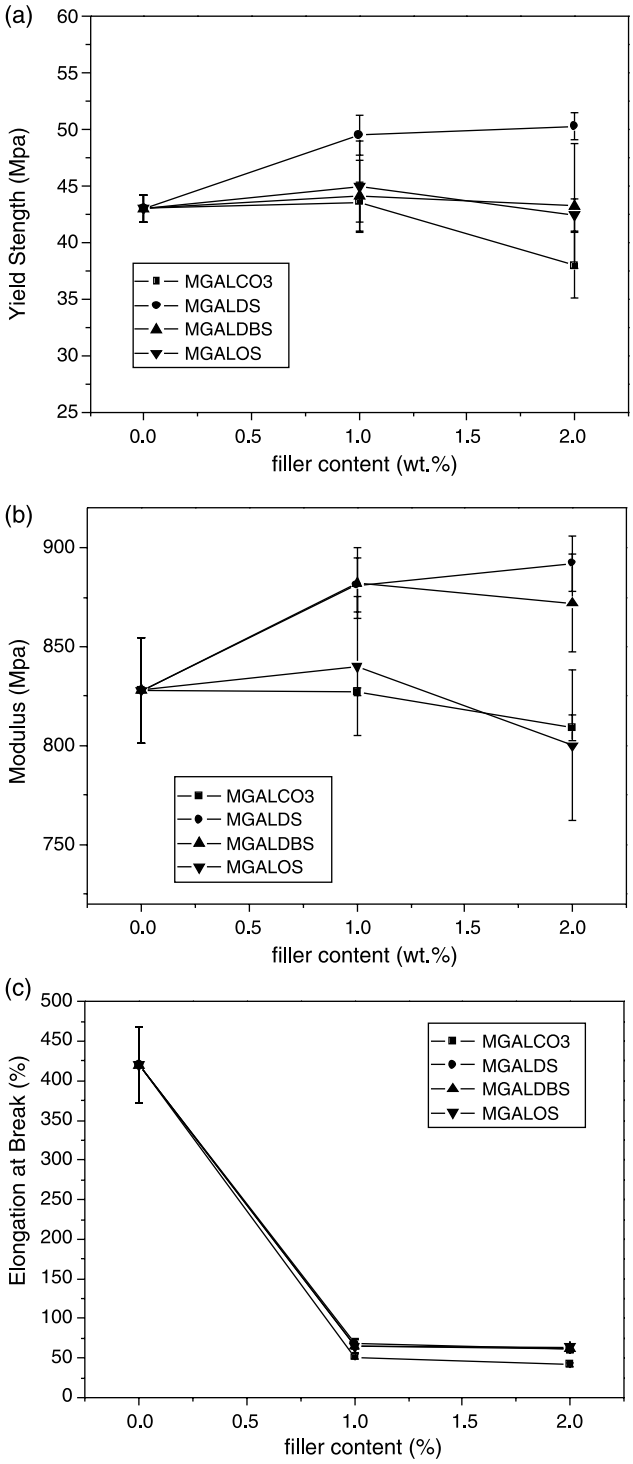

Fig. 9. (a) Yield strength, (b) modulus, and (c) elongation at break for PET nanocomposites at 50 °C.

1.27 with higher value of storage modulus at a low loss modulus value, indicating that the system is heterogeneity having filler–filler interactions. However, PET nanocomposites with 2.0 wt% MGALDS have lower slope value of about 0.87 than that of other nanocomposites, indicating presence of some network structures with filler–filler and filler–matrix interactions owing to the increased hydrophobic nature and exfoliated system of MGALDS. Over the loss modulus value of about 10^3, however, the slopes of curves for all nanocomposites increase and approach to homo PET curve whose slope is about 2.0. These results reflect that some network structures owing to filler–filler and/or filler–matrix interactions were collapsed by shear force, and became isotropic and homogeneous system [21]. Particularly, PET nanocomposite with MGALDS has similar storage modulus values with homo PET over the loss modulus value of 10^3, indicating more viscoelastic properties than other nanocomposites. The viscosity curves of nanocomposites are shown in Fig. 8(b). The viscosity curve of PET/MGALCO3 shows drastic shear thinning behavior because of the slip between polymer matrix and filler due to the lowest filler–matrix interaction. Although the viscosity of PET with MGALDBS, MGALDS, and MGALOS show also shear thinning behavior from a low frequency range, PET with MGALDBS and MGALOS draw continuous shear thinning curves due to the breakdown of network structure and slip between PET matrix and filler, while PET/MGALDS retains the viscosity like a homo PET at high frequency range owing to the increased filler–matrix interactions.

Fig. 9 shows mechanical properties of nanocomposites as a function of filler content. Young's modulus and yield stress for PET/MGALDS were increased with increasing filler content, because the exfoliation of the rigid LDH nanolayers in PET matrix directly enhanced the stiffness of nanocomposites. Those for PET with MGALDBS and MGALOS show same tendency with PET/MGALDS. However, when the DBS or OS content exceeds 1.0 wt%, the young's modulus and stress were decreased owing to the some aggregates of LDHs and decreased filler–matrix interactions. Young's modulus and stress for PET/MGALCO3 were also decreased with LDH content due to same reasons. However, elongation at break for all the nanocomposites was drastically decreased with LDH contents owing to the increased stiffness and micro-voids that were formed at around nanofillers during tensile testing.

4. Conclusions

Thermal, rheological, and mechanical properties of PET/LDH nanocomposites were investigated. DS, DBS, OS intercalated LDHs were successfully prepared by using rehydration mehod. MGALDS were exfoliated by PET molecules and dispersed well in PET matrix, resulting in increased thermal and mechanical properties. However, MGALDBS and MGALOS were not exfoliated efficiently. From the rheology study, there are some network structures owing to filler–filler and/or filler–matrix interactions in nanocomposite system. Consequently, MGALDS provided good compatibility with PET molecules, resulting in exfoliated MGALDS/PET nanocomposites having enhanced thermal and mechanical properties as compared to other nanocomposites as well as homo PET.

Acknowledgements

This work was supported by the next-generation new technology development project (#A18-05-07) of MOCIE.

References

[1] Ray SS, Okamoto M. Prog Polym Sci 2003;28:1539.
[2] Leroux F, Besse J. Chem Mater 2001;13:3507.
[3] Bubniak GA, Schreiner WH, Mattoso N, Wypych F. Langmuir 2002;18:5967.
[4] Hsueh HB, Chen CY. Polymer 2003;44:1151.
[5] Hsueh HB, Chen CY. Polymer 2003;44:5275.
[6] Costa FR, Abdel-Goad M, Wagenknecht U, Heinrich G. Polymer 2005;46:4447.
[7] Cavani F, Trifiro F, Caccari A. Catal Today 1991;11:173.
[8] Newman SP, Jones W. New J Chem 1998;22:105.
[9] Kohjiya S, Sato T, Nakayama T, Yamashita S. Macromol Rapid Commun 1981;2:231.
[10] Schaper H, Berg-Slot JJ, Stork WHJ. Appl Catal 1989;54:79.
[11] Pavan PC, Crepaldi EL, Gomes GD, Valim JB. Colloids Surf A 1999;154:399.
[12] Miyata S, Kumura T. Chem Lett 1973;843.
[13] Meyn M, Beneke K, Lagaly G. Inorg Chem 1990;29:5201.
[14] Schmassmann A, Tarnawski A, Flogerzi B, Sanner M, Varga L, Halter F. Eur J Gastroenterol Hepatol 1993;5:S111.
[15] Crepaldi EL, Pavan PC, Valim JB. J Mater Chem 2000;10:1337.
[16] Bish DL. Bull Mineral 1980;103:175.
[17] Chibwe K, Jones W. J Chem Soc, Chem Commun 1989;926.
[18] Chibwe K, Jones W. Chem Mater 1989;1:489.
[19] Dimotakis ED, Pinnavaia TJ. Inorg Chem 1990;29:2393.
[20] Chung SC, Hahm WG, Im SS, Oh SG. Macromol Res 2002;10:221.
[21] Han CD, Kim J, Kim JK. Macromolecules 1989;22:383.